Chalcogenide Letters Vol. 21, No. 7, July 2024, p. 529 - 541

Structural electronic and thermodynamic properties of CdX(X: S, Se, and Te) cadmium chalcogenides compound

A. Ouahab[a,*], L. Boudaoud[a], N. Boudaoud[b], H. Bradai[a], N. Hachemi[a], S. Menezla[c], N. Bounefla[a]

[a]*Energy, Environnement, and System Information Laboratory, Sciences and Technologies Faculty, Ahmed Draya University, Adrar, Algeria*

[b]*Polymer Materials Laboratory, Chemistry Faculty, University of Sciences and Technology HouariBoumediene, Algiers, Algeria*

[c]*Modeling and Simulation Laboratory in Materials Science (LMSSM), Faculty of Sciences, Djillali Liabes University, Sidi-Bel-Abbes, Algeria*

The structural and electronic properties of (CdS, CdSe, and CdTe) compounds in rock-salt, zinc-blend, and wurtzite crystal structures were calculated using ab initio calculation. In addition to these properties, the thermodynamic properties were added advantage to clarify their comportment as temperature variation. Under the context of density functional theory DFT, the calculations were carried out using the full potential linearized augmented plane wave FP-LAPW approach. The generalized gradient approximations GGA-PBE established by Perdew-Burke-Ernzerhof and the local density approximation LDA and modified Bucke Jhonson have both been employed for the exchange-correlation energy and related potential MBJ. The results show that the zinc-blend phases were the stable crystal structure for all compounds. The lowest direct band gap is found in the B3 phase for CdX, close to the experimental value. The values of band energies of CdS, CdSe, and CdTe were estimated to be 2,463 eV, 1,76 eV, and 1,532 eV, respectively. In general, this work fits well with other experimental and theoretical results. The quasiharmonic Debye theory is used to determine the impact of temperature and pressure on thermodynamic properties. This includes the calculation of pressure and temperature dependence, as well as the analysis of how heat capacity, thermal expansion, and the Debye temperature are affected by these variables.

(Received April 13, 2024; Accepted July 9, 2024)

Keywords: Ab-into, Structural properties, Chalcogenide, DFT, Properties electronic, MBJ

1. Introduction

The direct and fairly wide gap of VI semiconductors makes them crucial materials in today's technology. In light of the recent achievements in creating blue-green laser diodes, solar cells, and optoelectronic devices [1-4], there is a growing emphasis on understanding the physical characteristics of these compounds [5-7].

Cadmium chalcogenides were some of the first II-VI materials to be studied for semiconductor applications. It was recognized early on that their properties are similar to those of the more established III-V compounds. For example, the band gaps of the commonest zinc-blende compounds, CdS, CdSe, and CdTe are similar to those of the related III-V compounds GaP, GaAs, and GaSb [8-10]. The II-VI materials have an additional advantage in that they are much less prone to form native donors. This property has made them important materials for optoelectronic devices, and certain doped compositions are among the most successful infrared window materials. CdTe is also the material of choice for fabrication of nuclear radiation detectors and it is being intensively studied for solar cell applications [11]. Thus, it is difficult to overstate the importance of CdTe and the CdTe/CdS thin film solar cells [12, 13].

* Corresponding author: ouahab-ali@univ-adrar.edu.dz
https://doi.org/10.15251/CL.2024.217.529

The origin of interest in II-VI compounds is generally traced back to a paper by Dingle and Störmer addressing the potentially interesting semi magnetic behaviour of the II-Mn-VI magnetic semiconductors [14-16]. A resurgence of interest in recent years has been driven by discoveries in the field of diluted magnetic semiconductors [17].

This research aimed to compare various approximations of the full potential linearized augmented plane wave (FP-LAPW) approach within the density functional theory (DFT) framework. The objective was to analyze the structural and electronic properties and gain a deeper understanding of the thermodynamic properties. For the exchange and local potential correlation density approximation, the generalized gradient approximation (GGA) and the MBJ exchange potential were utilized. The use of the MBJ approximation enables the computation of energy band gaps for more accurate results, which align closely with experimental findings.

2. Computational methods

The FP-LAPW methodology, implemented in the (WIEN2k package), was utilized to calculate the structural and electronic properties of CdS, CdTe, and CdSe chalcogenide system. The GGA-PBE proposed by Perdew et al. was employed as the generalized gradient approximation, along with the LDA and mBJ exchange potential with the GGA approach for the calculation of electronic properties [18]. Throughout the calculations in the FP-LAPW scheme [19], as implemented in the WIEN2k computational code [20], consistent sphere radii and Kmax values were maintained for all lattice constants analyzed to ensure uniform convergence. The Fourier expanded charge density was truncated at Gmax=12. The total energy was determined until it reached a convergence of less than 10^{-3} Ry.

In order to analyze the thermodynamic characteristics of the CdS compound, we utilize the quasiharmonic Debye model, which has been extensively studied in previous research [21-24]. This model, incorporated into the Gibbs software [22, 25], takes into consideration how the material reacts to fluctuations in temperature and pressure. The expression for the non-equilibrium Gibbs function in this particular model is as presented in reference [23].

$$G^*(V,P,T) = E(V) + PV + \mathrm{A}_{Vib}[\theta_D(V),T] \tag{1}$$

where P is pressure, T is the Temperature, V is the volume, and A_{vib} is the non-equilibrium vibration Helmholtz free energy, θ_D is Debye temperature.
A_{Vib}can be given as:

$$\mathrm{A}_{Vib}[\theta_D(V),T] = NK_BT\left[\frac{9\theta_D}{8T} + 3\ln\left(1 - e^{\frac{-\theta_D}{T}}\right) - D(\frac{\theta_D}{T})\right] \tag{2}$$

where $D\left(\frac{\theta_D}{T}\right)$ is the Debye integral, (N) is the number of atoms per unit cell, (K_B) is the Boltzmann's constant. The details of the calculation can be found [26].

Moreover, for the heat capacities Cv and Cp at pressure and volume constant, respectively, and the coefficient of thermal expansion α may be determined using the following formulas:

$$C_v = 3NK\left[4D\left(\frac{\theta}{T}\right) - \frac{\frac{3\theta}{T}}{e^{D(\frac{\theta}{T})}-1}\right] \tag{3}$$

$$C_p = C_v(1 + \alpha\gamma T) \tag{4}$$

$$\alpha = \frac{\gamma C_v}{B_T V} \tag{5}$$

where γ is a Grüneisen parameter represented as:

$$\gamma = \frac{dln\theta(V)}{dlnV} \tag{6}$$

And B_T the isothermal bulk modulus, determined using the following formula:

$$B_T(P,T) = -V\left(\frac{\partial P}{\partial V}\right)_T \quad (7)$$

V is the equilibrium volume.

3. Results and discussion

3.1. Properties structural

The structural optimization for Zinc Blende, Rock-Salt, and Wurtzite crystal structure of (CdS, CdTe, and CdSe) compounds has been carried out using (GGA-PBE, GGA-WC, GGA-SOL, and LDA) Calculation by determining the minimum overall energy for different volumes of the unit cell. Moreover, the fitting of Murnaghan's Law [27] was used to optimize lattice parameters (a, c, u), Bulk modulus (B0), and derivate Bulk modulus (B0').

Figs (1 and 2) display the total energy versus volume curves. So, this section aims to compare the different approximations applied to the functional density theory. As it is shown in Fig.1, the lower total energies are obtained by the GGA-PBE potential. However, this approximation is the most accurate for our study. After that, the phase stability of our compounds is expected by the GGA-PBE correlation exchange potential. Fig. 2 illustrates all the minimized total energies as volumes of cells. The zinc blend presents the phase stability of all Cadmium chalcogenides compounds [28].

The summarized results of the calculations can be found in Table 1, which contains crystal structure data for the compounds analyzed in this investigation. These data are compared to both experimental and other theoretical values. Table 2 provides the various total energy values, highlighting the lowest values obtained from this study. Overall, this study aligns withprior theoretical and empirical discoveries.

Table 1. Illustrates many suggested structures' lattice parameters in Å, bulk modulus in GPa and dimensionless pressure derivative (CdS, CdTe, and CdSe).

PHASE		CdS				CdSe				CdTe			
		a	c	B	B'	a	c	B	B'	a	c	B	B'
ZB GGA-PBE	Present	5.945		54.113	4.576	6.200		45.216	4.669	6.619		35.276	4.975
LDA	Present	5.773		68.863	4.764	6.021		58.262	4.827	6.427		46.724	5.015
GGA-WC	Present	5.842		62.441	4.737	6.091		52.649	4.942	6.517		42.177	5.032
GGA-SOL	Present	5.839		62.541	4.980	6.100		53.470	5.059	6.507		41.438	4.802
	EXP	5.82[29]		62		6.05[29]		53		6.48[29]		44.5	
	Theory	5.80[1] 5.85[3] 5.818[30] 5.830[31]		70.3 70		6.07[32] 6.04[1] 6.05[30]		59.2 59.2	4.67	6.44[1] 6.40[3] 6.43[33]		46.6 52 46	
RS GGA-PBE	Present	5.502		75.196	3.982	5.739		60.591	4.902	6.125		46.59	4.863
LDA	Present	5.352		97.150	4.465	5.578		79.640	4.815	5.946		62.362	5.053
GGA-WC	Present	5.416		85.705	4.888	5.643		72.325	4.959	6.016		57.066	5.048
GGA-SOL	Present	5.413		85.512	4.821	5.640		71.719	4.942	6.004		56.028	4.761
	Theory	5.452[34] 5.321[32] 5.352[35] 5.43[36]		105 97.28	4.0 4.51	5.71[34] 5.49[36]				5.801[39]			
	EXP	5.441[37]				5.54[38]				5.59[40]			
WZ GGA-PBE	Present	4.187	6.799	53.954	4.859	4.403	7.11	43.983	5.263	4.689	7.657	35.728	5.021
	Theory	4.136[41] 4.086[42] 4.18[43] 4.136[44] 4.16[45]	6.597 6.768 6.683 6.753	68.9 79.48 99.52	4.70 2.94 4.0	4.13[47] 4.298[48]	6.92			4.582[49]	7.336		
	EXP	4.142[46]	6.723			4.30[36]	7.04			4.572[50]	7.484		

Table 2. The total energy for the different approximations (GGA-WC, GGA-PBE, and GGA-SOL) of (CdS, CdTe, and CdSe).

CdX		CdS			CdSe			CdTe		
Approximation		PBE	WC	SOL	PBE	WC	SOL	PBE	WC	SOL
Total Energy (Ry)	ZB	-11990,534	-11988,615	-11984,094	-16052,579	-16050,164	-16044,127	-24785,883	-24782,987	-24774,97
	RS	-11990,492	-11988,605	-11984,081	-16052,566	-16050,183	-16044,115	-24785,869	-24782,972	-24774,92
	WZ	-11990,495	-11988,575	-11984,092	-16052,578	-16050,162	-16044,128	-24785,881	-24782,942	-24774,969

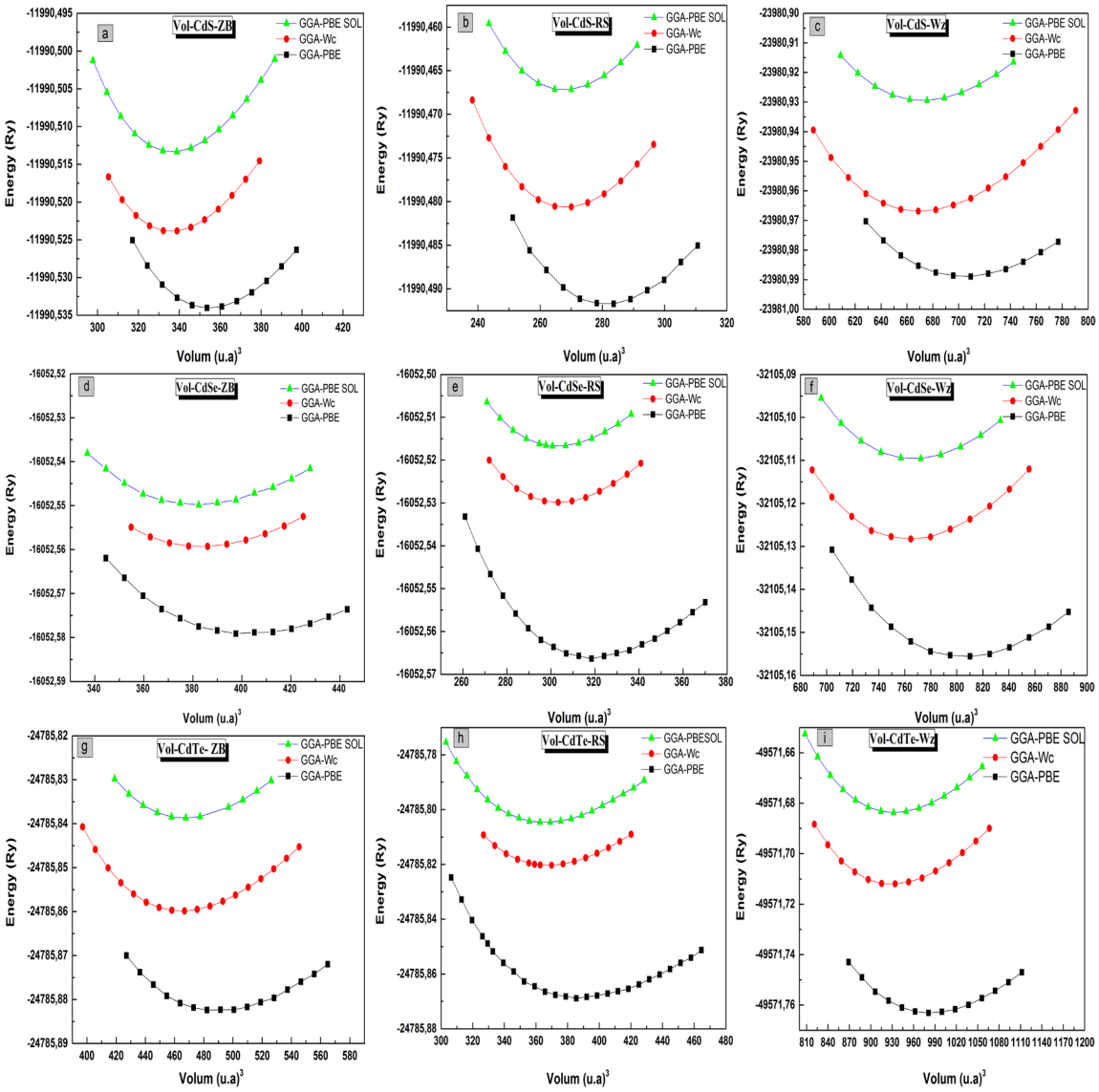

Fig. 1. The total energy versus cell volume for the different approximations (GGA-WC, GGA-PBE, and GGA-SOL) of (CdS, CdSe, and CdTe).

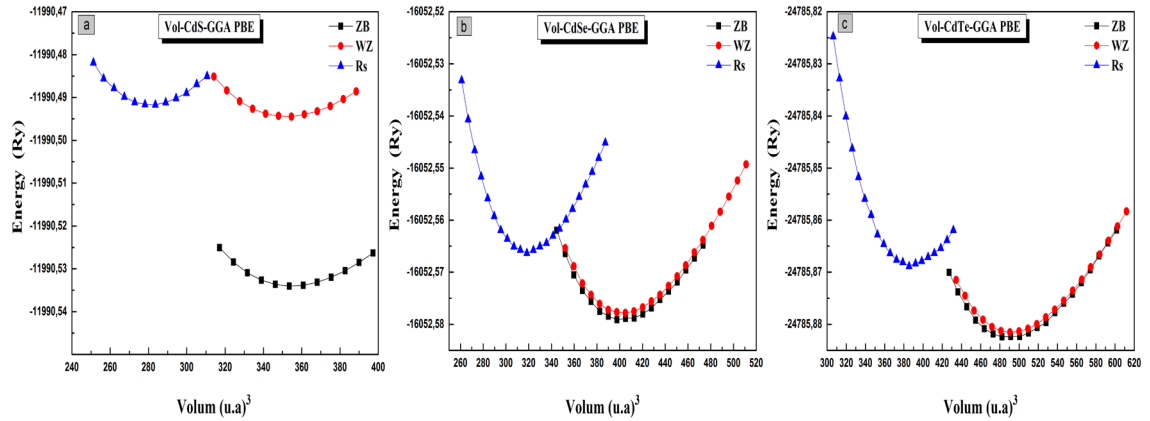

Fig. 2. The total energy versus cell volume for the different phases of (a: CdS, b: CdSe, and c: CdTe).

3.2. Properties electronic

After improving the crystal structure, we compute and analyze the crystal's electronic properties. Fig.3 depicts the estimated band structures (in the neighborhood of Fermi's level). First impressions of the computed bands show that all crystals are semiconductors due to a definite, well-defined band gap.

We studied the electronic structure of CdX. Fig.3 shows the power band diagram of (CdS, CdTe, and CdSe)-ZB calculated using GGA, LDA, and MBJ.

In Figure 3, it is evident that the conduction band minimum and valance band maximum are situated at the midpoint of the Brillouin zone, specifically at the point Γ. This positioning signifies that the band gap is a direct band gap. However, the calculated band gap using the LDA method and GGA method in Figure 3 is lower than the experimentally reported by O Madelung and all [29]. As a result, the LDA and GGA methods underestimate the energy band gap. For this resean, the MBJ-GGA is used for the band gap calculation. Figure 3 displays reasonable values obtained in agreement with the experimental value, with only a minor discrepancy. One explanation for this slight difference is the fact that the current calculation is conducted at absolute temperature, whereas the experimental value is measured at room temperature. Consequently, the GGA and LDA methods undervalue the energy band gap. Additionally, Figure 3 presents the band gap value calculated using the MBJ method, which aligns reasonably well with the experimentally reported values. Most importantly, the band gap value increases in the following order: LDA < GGA < MBJ.

Table 3 contains details on the chemicals examined in this work and compares them to experimental and other theoretical values that are currently accessible.

In order to gain a deeper understanding of the electronic arrangement of CdX, an analysis has been conducted on the overall and specific density of states DOS within the frameworks of GGA, LDA, and MBJ. The corresponding results can be observed in Figure 4.

Initially, the identification of the two lowest bands in the LDA calculation is denoted by the presence of the first lowest band. The contribution trend of the p-states (S, Se, Te) is MBJ > GGA > LDA, while the contribution trend of the d-t2g state (Cd atom) is also MBJ > GGA > LDA.

An intriguing piece of information concerning the state's involvement in the GGA, LDA, and MBJ is that the contribution trend of the s-state (S, Se, Te) exhibits the pattern of MBJ > GGA > LDA in the initial lowest band.

In the second lowest energy band, the d-eg-state (Cd atom) exhibits a contribution trend where MBJ surpasses GGA and LDA. Similarly, in the d-t2g state (Cd atom), MBJ takes precedence over GGA and LDA.

Consequently, the general tendency of the states in the valance band utilizing the three approaches is LDA<GGA<MBJ.

Consequently, the accurate findings of the MBJ computation come from treating the electronic states correctly.

Table 3. Shows the band gap energies of several proposed structures (CdS, CdSe, and CdTe).

			BPE	LDA	MBJ	EXP
CdX		Phase	direct Gap (eV)	direct Gap (eV)	direct Gap (eV)	Experimental (eV)
CdS	Present Theory	ZB	0,968 0.89[51] 1.15[52] 1.23[45] 1.21[46]	0,918 1.37 [3] 2.61[46]	2,463	2.55[29]
CdSe	Present Theory	ZB	0,431 0.33[51]	0,372 0.76[3] 2.65[46]	1,760	1.90[29] 1.93[53]
CdTe	Present Theory	ZB	0,546	0,567 0.80[3] 1.35[46]	1,532	1.60[29] 1.52[54]

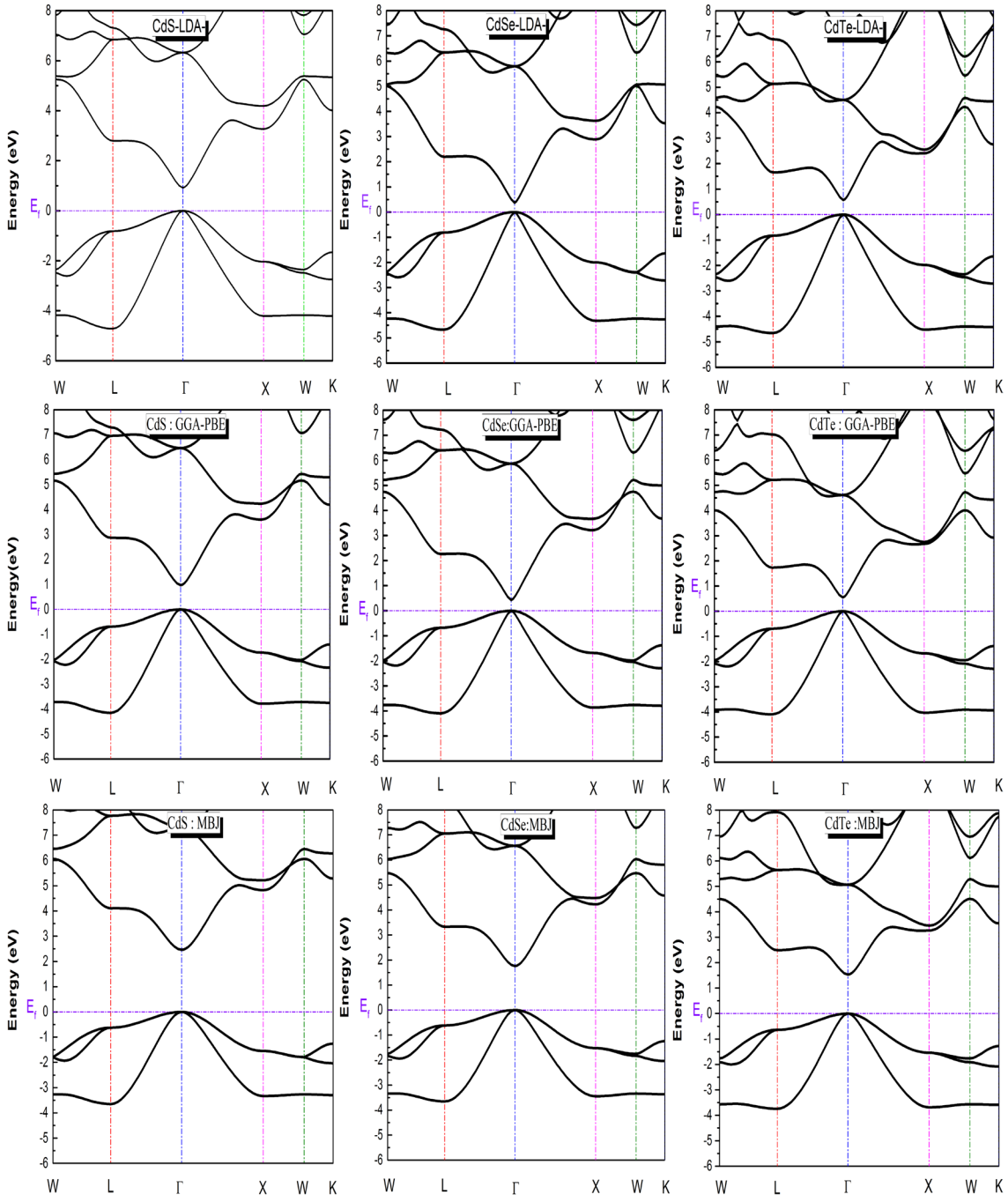

Fig. 3. Displays the computed band structures along the directions of higher symmetry in CdS. (zinc-blende), CdSe (zinc-blende), and CdTe (zinc-blende) within LDA, GGA, and MBJ-GGA.

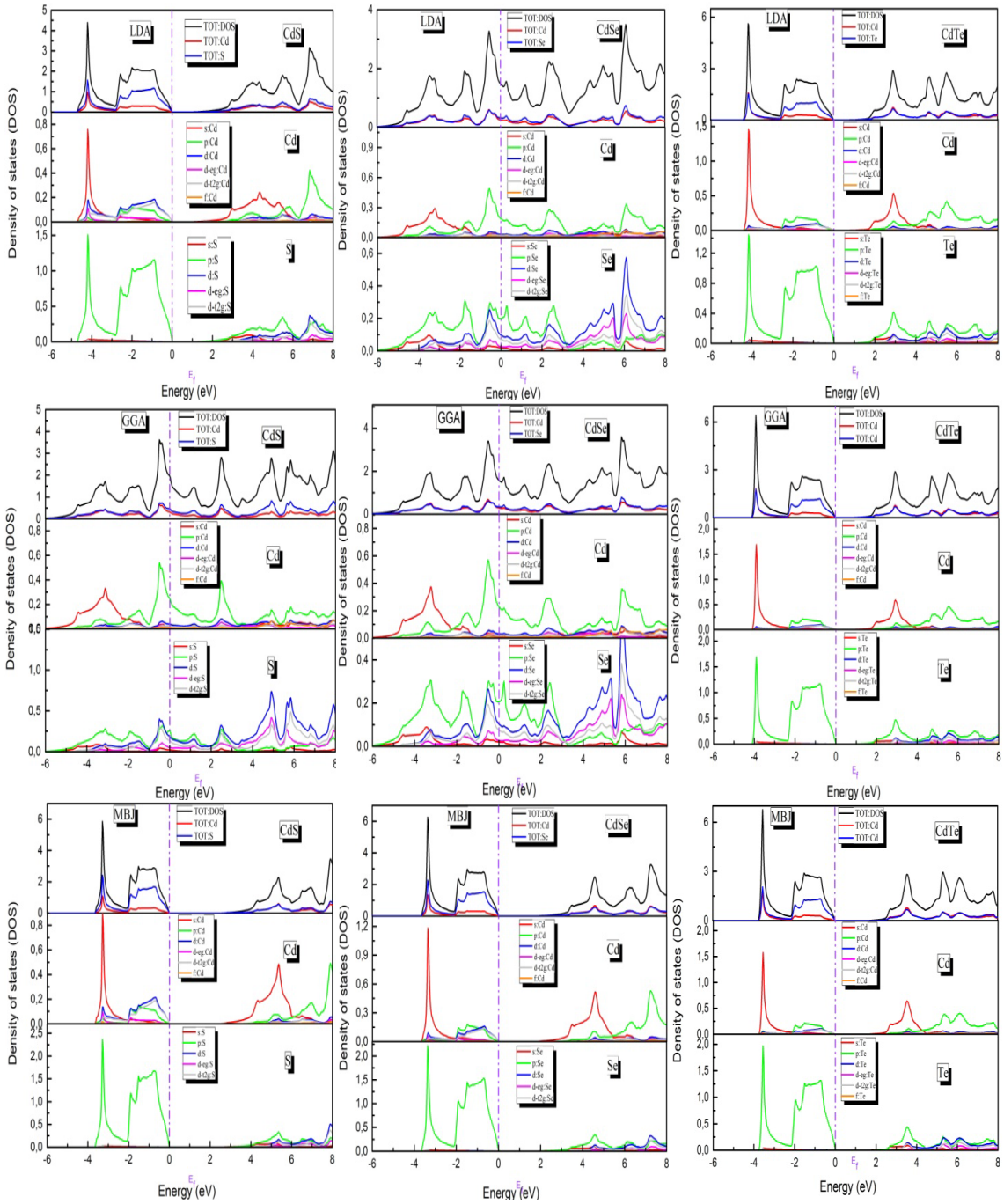

Fig. 4. Density of States (DOS) and partial states of CdS, CdSe and CdTe (ZB)within LDA,GGA and Mbj.

3.3. Thermodynamic properties

In this section, the Debye temperature, heat capacity, are simulated to unveil the thermodynamic characteristics. Temperature plays a crucial role in various physical properties, such as specific heat and thermal expansion. Both temperature and pressure range from 0 to 400K and 0 to 14 GPa respectively.

The graphical representation illustrating the relationship between the heat capacity at constant pressure, Cp(T), and constant volume, Cv(T), for different pressures of the material (CdS) is provided in Figure (5 and 6). It is observed that both Cv(T) and Cp(T) have values of zero at T = 0. The Debye model utilized here indicates that the shape of the curves is the same, and both Cv(T) and Cp(T) exhibit a substantial increase with rising temperature.

It is evident that the behavior of heat capacities follows a T^3 trend when the temperature is below the Debye temperature. This hyperbolic trend is particularly applicable when considering low oscillator frequencies. This principle holds true when the temperature satisfies the following condition: $T \leq \frac{\theta_D}{10}$ [24, 55].

At the Debye temperature, the specific heat capacity (Cp) was determined to be 49,374 J/mol.K. Under these conditions, oscillators are able to absorb thermal energy equivalent to thermal energy times Boltzmann constant (K_BT), resulting in the saturation of the excited oscillators. These oscillators exhibit harmonic behavior. As a result of this, the heat capacities remain consistent, while the number of phonons increases as the temperature rises. Additionally, if the temperature increases, the number of linear phonons also increases. And if $T > \theta_D$, the N linear

Nevertheless, the impact of anharmonicity on the constant volume heat capacity Cv(T) becomes negligible at elevated temperatures, causing Cv(T) to approach the Dulong-Petit limit [24, 55-61]. Conversely, when temperatures are sufficiently low, Cv(T) exhibits a direct relationship with T^3[61]. The heat capacity curve Cv(T) for CdS illustrates this behavior, with Cv(T) reaching the Dulong-Petit limit of 50,99628 J/mol.K at high temperatures. Additionally, at the Debye temperature, Cv is determined to be 47,735 J/mol.K.

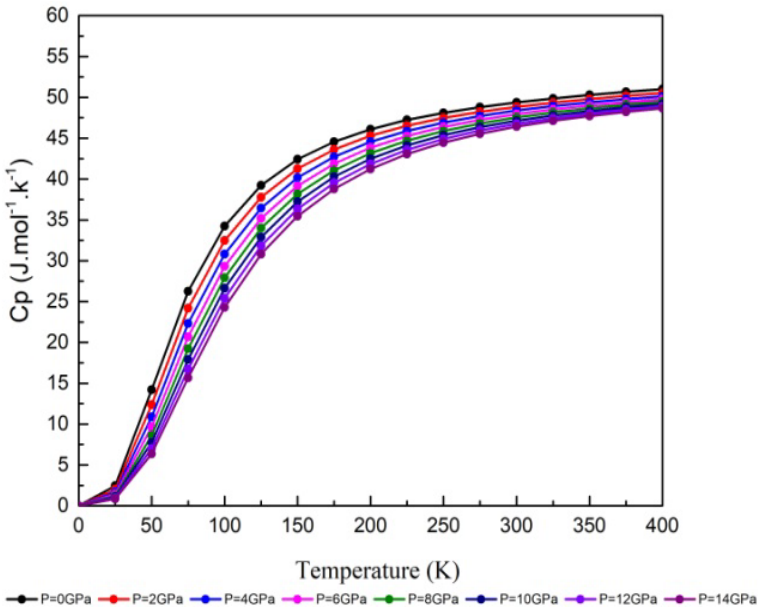

Fig. 5. Variation of the specific heat capacity with temperature under different pressure conditions.

According to the data presented in Figure 6, there is an observed increase in the heat capacity at constant pressure, denoted as Cv(T), as the temperature rises. Furthermore, this value does not reach a stable, constant value. Therefore, it would be of interest to raise the temperature beyond 400K in order to reach this limit.

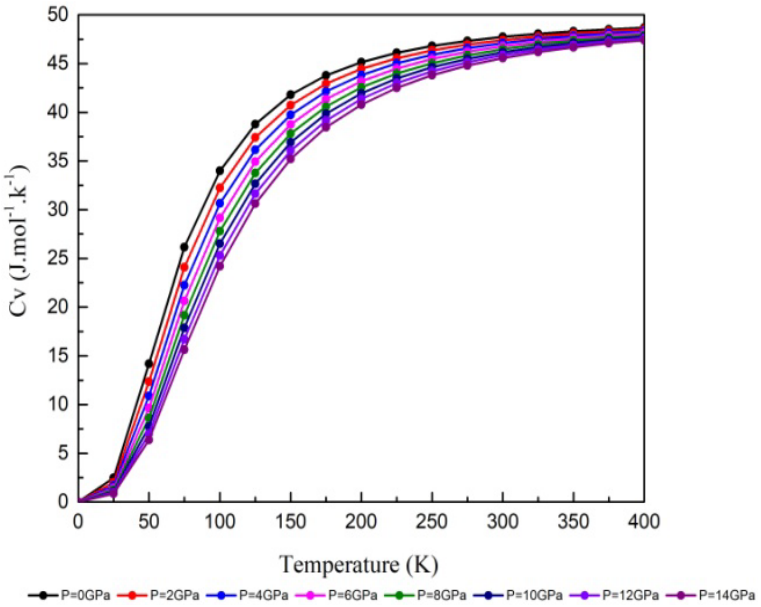

Fig. 6. Variation of heat capacity C_v with the temperature at different pressures.

In the realm of thermal vibrations superseding quantum effects, the Debey temperature (θ) emerges as the temperature at which the crystal exhibits conventional behavior, reflecting its maximum vibrational energy. Figure 7 show cases the progression of the Debye temperature (θ) in CdS material in relation to both temperature and pressure.

According to the data presented in this diagram, it can be observed that the value of (θ) remains relatively stable within the temperature range of 0 to 75 K, and gradually decreases in a linear manner as the temperature rises under different pressures. The estimated Debye temperature (θ) of CdS is reported to be 283 K when the temperature is 300K and the pressure is 0 GPa.

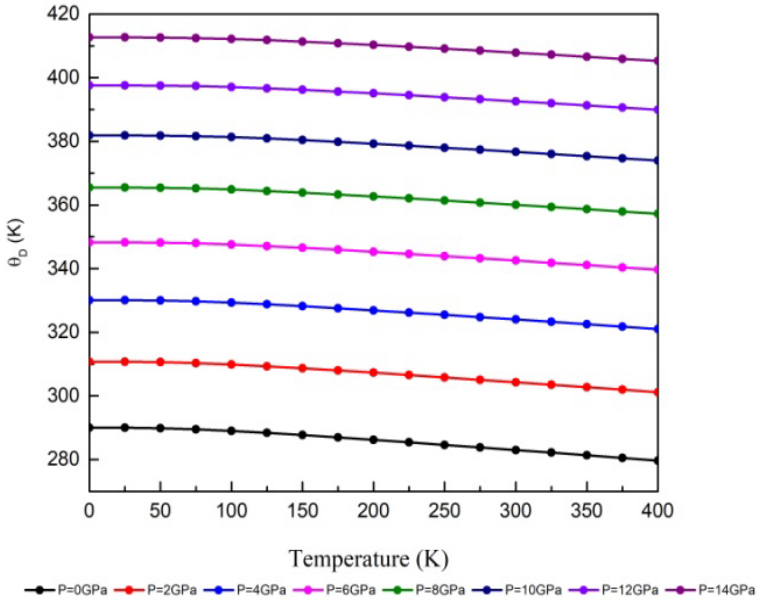

Fig. 7. The variation of the Debey temperature with temperature for distinct pressure values.

4. Conclusion

We presented and discussed the structure of the B1, B3, and B4 phases of CdX wide-gap semiconductor compounds in the framework of density functional theory using functional density theory with Linear augmented waves (FP-LAPW) potentials. Our GGA calculations show the Zinc blend as the stable phase of all compounds. The electronic band structures are given, and this compound has a semiconductor behavior with significant gaps in the phases studied in this paper. In general, this work fits well with the experimental results. The results of this study could offer valuable guidance for the utilization of CdX in various device applications, such as tandem solar cells, photoconductive detectors, and optoelectronic devices. To sum up, our findings serve as a reference for future research endeavors.

Acknowledgments

The authors would like to extend their gratitude to the Energy, Environnement, and System Information Laboratory, Sciences and Technologies Faculty, Ahmed Draya University

References

[1] S.-H. Wei, S. Zhang, Physical review B, 62, 6944 (2000); https://doi.org/10.1103/PhysRevB.62.6944

[2] B. Rajput, D. Browne, Physical Review B, 53, 9052 (1996); https://doi.org/10.1103/PhysRevB.53.9052

[3] O. Zakharov, A. Rubio, X. Blase, M.L. Cohen, S.G. Louie, Physical Review B, 50, 10780 (1994); https://doi.org/10.1103/PhysRevB.50.10780

[4] R. Nelmes, M. McMahon, in: Semiconductors and semimetals, Elsevier, pp. 145-246 (1998); https://doi.org/10.1016/S0080-8784(08)60231-8

[5] J. Shi, J. Zhang, L. Yang, M. Qu, D.C. Qi, K.H. Zhang, Advanced materials, 33, 2006230 (2021); https://doi.org/10.1002/adma.202006230

[6] R. Woods-Robinson, Y. Han, H. Zhang, T. Ablekim, I. Khan, K.A. Persson, A. Zakutayev, Chemical reviews, 120, 4007-4055 (2020); https://doi.org/10.1021/acs.chemrev.9b00600

[7] Z. Li, T. Yan, X. Fang, Nature Reviews Materials, 8, 587-603 (2023); https://doi.org/10.1038/s41578-023-00583-9

[8] J. Li, X. Zhou, Journal of Physics D: Applied Physics, 54, 415104 (2021); https://doi.org/10.1088/1361-6463/ac1374

[9] E.G. LeBlanc, Texas State University-San Marcos, (2020).

[10] W. Pan, Z. Zhang, J. Liu, W. Lei, L. Faraone, nfrared Physics & Technology, 111, 103522 (2020); https://doi.org/10.1016/j.infrared.2020.103522

[11] T. Takahashi, S. Watanabe, IEEE Transactions on nuclear science, 48, 950-959 (2001); https://doi.org/10.1109/23.958705

[12] A.B. Phillips, J.D. Friedl, K.K. Subedi, Z. Song, R.H. Ahangharnejhad, A. Abudulimu, E. Bastola, I. Subedi, M.K. Jamarkattel, Z. Hussain, Solar Energy Materials and Solar Cells, 266, 112689 (2024); https://doi.org/10.1016/j.solmat.2023.112689

[13] K.C. Nwambaekwe, V.S. John-Denk, S.F. Douman, P. Mathumba, S.T. Yussuf, O.V. Uhuo, P.I. Ekwere, E.I. Iwuoha, journal of materials research and technology, 12, 1252-1287 (2021); https://doi.org/10.1016/j.jmrt.2021.03.047

[14] W. Nunn, T.K. Truttmann, B. Jalan, Journal of materials research, 1-19 (2021).

[15] A.Einstein, B. Podolsky, and N. Rosen, Phys. Rev. 47, 777-780 (1935); https://doi.org/10.1103/PhysRev.47.777

[16] D. Kudlacik, K. Kavokin, C. Lüders, K. Barthelmi, J. Schindler, H. Moldenhauer, P.

Waldkirch, V. Sapega, D. Yakovlev, A. Waag, Physical Review B, 101, 155432 (2020); https://doi.org/10.1103/PhysRevB.101.155432
[17] S. Ram, H. Aldarmaki, arXiv preprint arXiv:2301.01020, (2023).
[18] J.P. Perdew, K. Burke, M. Ernzerhof, Physical review letters, 77, 3865 (1996); https://doi.org/10.1103/PhysRevLett.77.3865
[19] O.K. Andersen, Physical Review B, 12, 3060 (1975); https://doi.org/10.1103/PhysRevB.12.3060
[20] P. Blaha, K. Schwarz, G.K. Madsen, D. Kvasnicka, J. Luitz, An augmented plane wave+ local orbitals program for calculating crystal properties, 60 (2001).
[21] P. Debye, Annalen der Physik, 344, 789-839 (1912); https://doi.org/10.1002/andp.19123441404
[22] M. Blanco, E. Francisco, V. Luana, Computer Physics Communications, 158, 57-72 (2004); https://doi.org/10.1016/j.comphy.2003.12.001
[23] A. Otero-de-la-Roza, D. Abbasi-Pérez, V. Luaña, Computer Physics Communications, 182, 2232-2248 (2011); https://doi.org/10.1016/j.cpc.2011.05.009
[24] A. Otero-de-la-Roza, V. Luaña, Computer Physics Communications, 182, 1708-1720 (2011); https://doi.org/10.1016/j.cpc.2011.04.016
[25] M.A. Blanco, Universidad de Oviedo, (1997).
[26] T. Yang, J. Cao, X. Wang, Crystals, 8, 429 (2018); https://doi.org/10.3390/cryst8110429
[27] F.D. Murnaghan, Proceedings of the National Academy of Sciences, 30, 244-247 (1944); https://doi.org/10.1073/pnas.30.9.244
[28] O. Ali, B. Lahouaria, Physica Scripta, 99, 045922 (2024); https://doi.org/10.1088/1402-4896/ad2e53
[29] O. MADELUNG, Landolt Bornstein, New Series, Group III, 22, 117 (1982).
[30] R.K. Willardson, E.R. Weber, W. Paul, T. Suski, Academic Press, (1998).
[31] R.T. Shannon, C.T. Prewitt, Acta Crystallographica Section B: Structural Crystallography and Crystal Chemistry, 25, 925-946 (1969); https://doi.org/10.1107/S0567740869003220
[32] N. Benkhettou, D. Rached, B. Soudini, M. Driz, physica status solidi (b), 241, 101-107 (2004); https://doi.org/10.1002/pssb.200301907
[33] M. Kanoun, W. Sekkal, H. Aourag, G. Merad, Physics Letters A, 272, 113-118 (2000); https://doi.org/10.1016/S0375-9601(00)00403-5
[34] J.N. Wickham, A.B. Herhold, A. Alivisatos, Physical Review Letters, 84, 923 (2000); https://doi.org/10.1103/PhysRevLett.84.923
[35] Y. Li, X. Zhang, H. Li, X. Li, C. Lin, W. Xiao, J. Liu, Journal of Applied Physics, 113 (2013); https://doi.org/10.1063/1.4792233
[36] A. Mariano, E. Warekois, Science, 142, 672-673 (1963); https://doi.org/10.1126/science.142.3593.672
[37] R. Miller, F. Dachille, R. Roy, Journal of Applied Physics, 37, 4913-4918 (1966); https://doi.org/10.1063/1.1708164
[38] C. Rooymans, Physics Letters, 4, 186-187 (1963); https://doi.org/10.1016/0031-9163(63)90356-1
[39] J.Z. Hu, Solid state communications, 63, 471-474 (1987); https://doi.org/10.1016/0038-1098(87)90273-0
[40] I. Borg, D. Smith Jr, Journal of Physics and Chemistry of Solids, 28, 49-53 (1967); https://doi.org/10.1016/0022-3697(67)90196-5
[41] W.R. Cook JR, Journal of the American Ceramic Society, 51, 518-520 (1968); https://doi.org/10.1111/j.1151-2916.1968.tb15678.x
[42] K. Wright, J.D. Gale, Physical Review B, 70, 035211 (2004); https://doi.org/10.1103/PhysRevB.70.035211
[43] M. Knudson, Y. Gupta, A. Kunz, Physical Review B, 59, 11704 (1999);

https://doi.org/10.1103/PhysRevB.59.11704
[44] K. Susa, T. Kobayashi, S. Journal of Solid State Chemistry, 33, 197-202 (1980); https://doi.org/10.1016/0022-4596(80)90120-6
[45] A. Andreev, M. Bulanyi, S. Golikov, L. Mozharovskii, Russian journal of inorganic chemistry, 40, 1039-1042 (1995).
[46] F. Ulrich, W. Zachariason, Z. Kristallogr, 62, 260-273 (1925); https://doi.org/10.1524/zkri.1925.62.1.260
[47] M.L. Cohen, J.R. Chelikowsky, IV-VI Semiconductors, Electronic Structure and Optical Properties of Semiconductors, 172-188 (1988); https://doi.org/10.1007/978-3-642-97080-1_11
[48] A. Al-Bassam, A. Al-Dhafiri, Journal of crystal growth, 134, 63-66 (1993); https://doi.org/10.1016/0022-0248(93)90009-L
[49] I. Dima, D. Borşan, physica status solidi (b), 23, K113-K115 (1967); https://doi.org/10.1002/pssb.19670230242
[50] I. Spinulescu-Carnaru, physica status solidi (b), 15, 761-765 (1966); https://doi.org/10.1002/pssb.19660150237
[51] A. Boukortt, S. Berrah, R. Hayn, A. Zaoui, Physica B: Condensed Matter, 405, 763-769. (2010); https://doi.org/10.1016/j.physb.2009.09.102
[52] D. Rodic, V. Spasojevic, A. Bajorek, P. Onnerud, Journal of magnetism and magnetic materials, 152, 159-164 (1996); https://doi.org/10.1016/0304-8853(95)00435-1
[53] M. H. Mustafa, H. M. Ali, G. S. Ahmed, B. H. Hussein, Chalcogenide Letters, 2010, 733-740 (2023); https://doi.org/10.15251/CL.2023.2010.733
[54] H. M. Ali, M. H. Mustafa, Chalcogenide Letters, 206, 431-437 (2023); https://doi.org/10.15251/CL.2023.206.431
[55] V. Srivastava, N. Kaur, R. Khenata, S.A. Dar, Journal of Magnetism and Magnetic Materials, 513, 167107 (2020); https://doi.org/10.1016/j.jmmm.2020.167107
[56] S. Al-Qaisi, M. Abu-Jafar, G. Gopir, R. Khenata, Phase Transitions, 89, 1155-1164 (2016); https://doi.org/10.1080/01411594.2016.1156111
[57] H. Pawar, M. Aynyas, S.P. Sanyal, Journal of Magnetism and Magnetic Materials, 468, 123-131 (2018); https://doi.org/10.1016/j.jmmm.2018.07.085
[58] S.N. Tripathi, V. Srivastava, R. Khenata, S. Sanyal, Computational Condensed Matter, 28, e00563 (2021); https://doi.org/10.1016/j.cocom.2021.e00563
[59] S.A. Dar, R. Sharma, V. Srivastava, U.K. Sakalle, RSC Adv. 9, 9522 (2019); https://doi.org/10.1039/C9RA00313D
[60] A. Petit, P. Dulong, Ann. Chem. Phys, 10, 395 (1981).
[61] E. Andritsos, E. Zarkadoula, A. Phillips, M. Dove, C. Walker, V. Brazhkin, K. Trachenko, Journal of Physics: Condensed Matter, 25, 235401 (2013); https://doi.org/10.1088/0953-8984/25/23/235401